

Time-Optimal Control and Parameter Estimation of Diafiltration Processes in the Presence of Membrane Fouling

Martin Jelemenský* Martin Klaučo* Radoslav Paulen**
Joost Lauwers*** Filip Logist*** Jan Van Impe***
Miroslav Fikar*

* *Slovak University of Technology in Bratislava, Slovakia, (e-mail: {martin.jelemensky, martin.klauco, miroslav.fikar}@stuba.sk).*

** *Technische Universität Dortmund, Germany, (e-mail: radoslav.paulen@bci.tu-dortmund.de)*

*** *Katholieke Universiteit Leuven, Belgium, (e-mail: {joost.lauwers, filip.logist, jan.vanimpe}@cit.kuleuven.be).*

Abstract: This paper deals with the time-optimal operation and parameter estimation problem of a general diafiltration process in the presence of fouling. Fouling stands for one of the dominant problems in the membrane separation processes. The dynamic behavior of the fouled membrane is described by a general fouling model taken from literature. An Extended Kalman filter is proposed for the recursive estimation of unknown parameters in the fouling model. A model-based optimal nonlinear controller, whose control law is obtained explicitly via Pontryagin's minimum principle, is coupled with the parameter estimation and subsequently applied in a simulation case study to show benefits of the proposed approach.

Keywords: Kalman filter, batch diafiltration, optimal control, membrane fouling, parameter estimation

1. INTRODUCTION

Membrane processes employ perm-selective membranes to separate solutes in a solution based on differences in molecular size so that the high molecular weight components are retained on the feed side of the membrane and the low molecular weight components are able to pass through it. These processes have found a wide range of application in the pharmaceutical, food, and biotechnological industries (Cheryan, 1998).

A diafiltration is a membrane process that uses a solute-free solvent (diluant) to control the membrane process via influencing the concentrations of solutes. Several authors (Foley, 1999; Takači et al., 2009) showed that different strategies of diluant addition can result in different operational savings where time-optimal operation or minimal consumption of diluant can be achieved.

Ng et al. (1976); Takači et al. (2009); Paulen et al. (2012) optimized the final processing time and/or the consumption of the diluant. This includes the optimization of the switching times between the predefined operational modes, such as concentration, constant-volume diafiltration, application of sophisticated numerical and analytical approaches. Our recent work (Paulen et al., 2015) showed that the two major optimization problems can be solved as a single optimization problem formulated in a multi-objective fashion where a use of Pontryagin's minimum principle allows to obtain analytical solutions for many common process setups.

Fouling behavior is one of main issues in membrane separation processes. It decreases effective membrane area due to the blockage of pores and results in a substantial increase of operational costs. The pioneering work of Hermia (1982) presented a unified fouling model describing this behavior. Recently, Charfi et al. (2012) showed that numerical optimization techniques can be employed to predict types of the fouling mechanism using experimental data of the permeate flow.

In the work of Jelemenský et al. (2015b) the authors derived a fully analytical procedure for the time-optimal operation in the presence of the membrane fouling. However, optimal model-based control of membrane processes proposed also by Paulen et al. (2015); Jelemenský et al. (2015a) requires a knowledge of process model and its parameters where the use of inaccurate values of the parameters could lead to significantly suboptimal performance. Estimation of unknown parameters can be done using various methods. Common practice is to employ a least-squares method off-line. More advanced methods include Kalman filtering or moving horizon estimation strategies (Alessandri et al., 2005).

In this paper we study the combined time-optimal operation of a batch diafiltration process and the estimation of fouling parameters using Extended Kalman Filter (EKF). The proposed scheme is attractive as it applies inherently robust nonlinear optimal feedback control with on-line estimation of process parameters. We will show that the estimation of the fouling behavior results in optimal con-

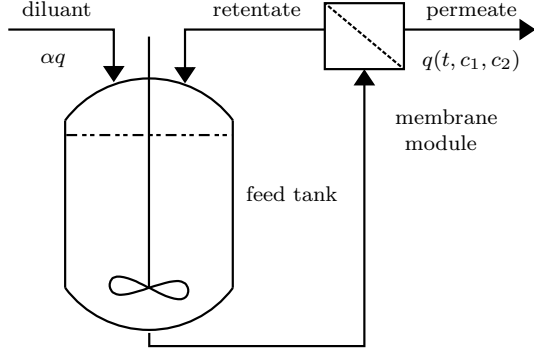


Fig. 1. Schematic representation of a generalized diafiltration process.

control performance even if the fouling parameters are initially not known.

The paper is organized as follows. Section 2 describes the process and its model including a model of fouling behavior. Section 3 presents the formulation of the optimization problem and its analytical solution. An overview of EKF and its application to the studied problem is described in Section 4. The proposed approach is applied in a simulation study in Section 5. Section 6 concludes the paper.

2. PROCESS DESCRIPTION AND MODELING

In this paper we study a generalized batch diafiltration process represented in Fig. 1. We consider that the process runs under constant pressure and temperature. The diafiltration process involves a feed tank, where the solution that consist of two solutes is introduced, and a membrane. The feed is brought to the membrane and the stream rejected by the membrane (retentate) is taken back into the feed tank. The stream which leaves the system is called permeate and its flow-rate is defined as $q = AJ$, where A is the membrane area and J is the permeate flux subject to unit membrane area. The permeate flux can be a function of solutes concentrations and time.

The control of the diafiltration process can be achieved by adding a solute-free solvent (diluant) into the feed tank. The control variable α expresses the ratio between the inflow of diluant and the outflow of the permeate q . In the industry, there are traditionally used control modes which differ in the rate of diluant addition. A mode with $\alpha = 0$, during which no diluant is added into the feed tank, is called concentration (C) mode. The second traditional mode is constant-volume diafiltration (CVD) where $\alpha = 1$ and during this mode the inflow of diluant is kept the same as the permeate outflow. Dilution (D) mode is characterized by $\alpha = \infty$ where a certain amount of diluant is added into the feed tank. A typical industrial control strategy consists of a sequence of the aforementioned control modes (e.g. C-CVD).

The mass balance for the individual solutes can be written as (Kovács et al., 2009)

$$\frac{dc_i}{dt} = \frac{c_i q}{V} (R_i - \alpha), \quad c_i(0) = c_{i,0}, \quad i = 1, 2, \quad (1)$$

where V stands for the volume of the feed at time t and subscript i denotes the macro-solute and micro-solute,

respectively. R_i is the so-called rejection coefficient. The rejection coefficient is a dimensionless number between 0 and 1 that measures the ability of the membrane to reject a particular solute.

The total mass balance can be written as

$$\frac{dV}{dt} = u - q = (\alpha - 1)AJ, \quad V(0) = V_0, \quad (2)$$

with V_0 being the initial volume of the processed solution.

Moreover, the rejection coefficient R_i can be a constant or a function of both concentrations. In the remainder of the paper we will consider that the rejection coefficients are constant ($R_1 = 1$ and $R_2 = 0$). This means that the membrane is perfectly impermeable for the macro-solute and that the micro-solute can freely pass through the membrane pores. Since the rejection for the macro-solute is equal to one, the total mass in the system will not change and stays constant ($c_1(t)V(t) = c_{1,0}V_0$). This allows us to eliminate the differential equation for the volume (2). Then, the equivalent model has the following form

$$\frac{dc_1}{dt} = \frac{c_1^2 AJ}{c_{1,0} V_0} (1 - \alpha), \quad c_1(0) = c_{1,0}, \quad (3)$$

$$\frac{dc_2}{dt} = -\frac{c_1 c_2 AJ}{c_{1,0} V_0} \alpha, \quad c_2(0) = c_{2,0}. \quad (4)$$

2.1 Membrane Fouling

The membrane fouling depends on several properties such as feed concentration and viscosity, membrane material, temperature, and pressure. Fouling causes the decrease of the effective membrane area due to the deposit of the solutes in/on the membrane. A unified model of the fouling behavior was derived by Hermia (1982) in terms of the total permeate flux and time and reads as

$$\frac{d^2 t}{dV_p^2} = K \left(\frac{dt}{dV_p} \right)^n, \quad (5)$$

where V_p represents the permeate volume, t is time, and K is the fouling rate constant. The parameter n determines the type of the fouling mechanism where four classical fouling models can be recognized: cake ($n = 0$), intermediate ($n = 1$), standard (internal) ($n = 3/2$), and complete ($n = 2$) fouling model.

Equation (5) can be rewritten as as (Bolton et al., 2006; Vela et al., 2008)

$$\frac{dJ}{dt} = -KA^{2-n}J^{3-n}. \quad (6)$$

and it can be solved for a particular choice of n to yield

$$n = 0 : \quad \frac{1}{J^2} = \frac{1}{J_0^2} + K_g t, \quad (7a)$$

$$n = 1 : \quad \frac{1}{J} = \frac{1}{J_0} + K_i t, \quad (7b)$$

$$n = \frac{3}{2} : \quad \frac{1}{\sqrt{J}} = \frac{1}{\sqrt{J_0}} + K_s t, \quad (7c)$$

$$n = 2 : \quad \ln J = \ln J_0 - K_c t, \quad (7d)$$

where J_0 is the initial flux and K_g, K_i, K_s, K_c are respective fouling constants for the different values of n .

Fig. 2 shows a graphical representation of these fouling mechanisms. The distinguishing feature of the models

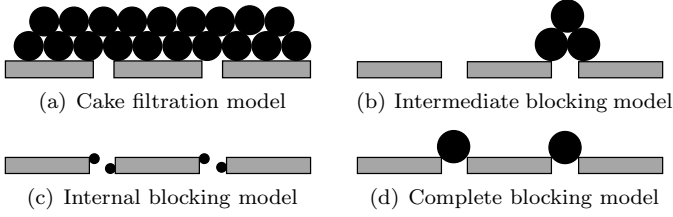


Fig. 2. Graphical representation of the four classical fouling models developed by Hermia (1982).

is present by the way the molecules deposit in/on the membrane. The complete pore blocking model considers that all solutes brought to the surface of the membrane will block all membrane pores. The intermediate fouling model assumes that not all solutes block the membrane surface and that the solutes can deposit on each other. The internal blocking model considers fouling in the membrane pores. The cake filtration model assumes that the solutes brought to the membrane will deposit on each other and form a filtration cake on the surface of the membrane.

Although the Hermia's model was derived for dead-end systems, we will apply it to cross-flow systems. Then, $J_0(c_1, c_2)$ will represent flux through the unfouled membrane and $J(t, c_1, c_2)$ the flux subject to fouling.

3. PROCESS OPTIMIZATION

The objective of the process optimization is to drive the process from the initial state defined by initial concentrations $c_{1,0}$ and $c_{2,0}$ to the desired final state $[c_1(t_f), c_2(t_f)]$ in a minimum time. The manipulated variable is $\alpha(t)$. The mathematical representation of the optimization problem is of the form

$$\mathcal{J}^* = \min_{\alpha(t)} \int_0^{t_f} 1 dt, \quad (8a)$$

s.t.

$$\dot{c}_1 = \frac{c_1^2 A J}{c_{1,0} V_0} (1 - \alpha), \quad c_1(0) = c_{1,0}, \quad (8b)$$

$$\dot{c}_2 = -\frac{c_1 c_2 A J}{c_{1,0} V_0} \alpha, \quad c_2(0) = c_{2,0}, \quad (8c)$$

$$c_1(t_f) = c_{1,f}, \quad (8d)$$

$$c_2(t_f) = c_{2,f}, \quad (8e)$$

$$J = J(t, J_0(c_1, c_2), K, n), \quad (8f)$$

$$\alpha \in [0, \infty). \quad (8g)$$

The optimization problem can be solved using various numerical or analytical methods of dynamic optimization.

In our recent paper (Jelemenský et al., 2015a) we derived the optimal operation of a diafiltration process subject to membrane fouling. Analytical approach based on Pontryagin's minimum principle (Pontryagin et al., 1962; Bryson, Jr. and Ho, 1975) was used. The optimal control is an explicit nonlinear control strategy defined on several concentration regions and over three consecutive time steps. The three steps are as follows.

- (1) In the first step a maximum or minimum control action is applied until the singular curve is reached

$$S(t, c_1, c_2) = J + c_1 \frac{\partial J}{\partial c_1} + c_2 \frac{\partial J}{\partial c_2} = 0. \quad (9)$$

If the initial state of the process lies to the left of the singular curve in the state diagram, the process is operated in concentration mode ($\alpha = 0$). In the opposite case, the process is operated in dilution mode ($\alpha = \infty$). Thus, the singular curve forms a border between different state regions.

- (2) The singular control is applied once the process state resides on the singular curve which forces the states to move along at the singular curve.

$$\alpha(t) = \frac{\frac{\partial S}{\partial c_1} c_1}{\frac{\partial S}{\partial c_1} c_1 + \frac{\partial S}{\partial c_2} c_2} + \frac{\frac{\partial S}{\partial t}}{\frac{c_1 A J}{c_{1,0} V_0} \left(\frac{\partial S}{\partial c_1} c_1 + \frac{\partial S}{\partial c_2} c_2 \right)}. \quad (10)$$

This step is terminated once the ratio of the concentrations is equal to the ratio of their final concentrations or when the desired concentration of micro-solute is reached.

- (3) The last step is similar to the first step. The position of the final state point decides whether we apply the concentration mode with $\alpha = 0$ (this is done when the final point lies to the right of the singular curve) or the pure dilution mode with $\alpha = \infty$ (this is the case when the final point lies to the left of the singular curve) until the final concentrations are reached.

Note that the optimal control does not depend on the fouling model and the fouling constant in the first and the last step. This property is used in the proposed methodology as it helps to retain optimality even if the process model is initially not known perfectly.

The optimal sequence of operations depends on the initial and final states. Therefore, any of the steps can be missing from the optimal control structure. For example, the singular step can be skipped and the optimal control will be saturated on constraints for a particular set of initial and final conditions.

4. PARAMETER ESTIMATION

As presented above the membrane fouling belongs to one of main obstacles in membrane separation since it causes the membrane flux to decline. Another issue is that the fouling behavior can change with time. Several fouling mechanisms can occur in parallel or in series during the run of process. For example Abbasi et al. (2012) have observed experimentally different fouling phenomena during one batch. Salahi et al. (2010) have described experiments where the initial flux decline was attributed to standard pore blocking mechanism and changed to cake formation in the final phase.

Therefore, to achieve better performance of the membrane separation it is necessary to estimate not only the values of the individual fouling constants but also the fouling model itself. This can be achieved by employing an Extended Kalman Filter (Kalman, 1960; Bavdekar et al., 2011) (EKF) for the simultaneous estimation of states and parameters. Main parameters that are necessary to obtain accurate information about fouling are the fouling constant K and the parameter n .

The main idea behind the EKF is that the non-linear system is linearized around the current EKF estimate and

the measurements are taken at discrete time instants in order to correct the dynamics of the filter.

In the first step it is necessary to augment the vector of state variables with the estimated parameters θ that represent new states with no dynamics and unknown initial value. Further, the explicit appearance of time is replaced by a new state x_3 , yielding new process description with 5 states

$$\dot{c}_1 = \frac{c_1^2 A J}{c_{1,0} V_0} (1 - \alpha), \quad c_1(0) = c_{1,0}, \quad (11a)$$

$$\dot{c}_2 = -\frac{c_1 c_2 A J}{c_{1,0} V_0} \alpha, \quad c_2(0) = c_{2,0}, \quad (11b)$$

$$\dot{x}_3 = 1, \quad x_3(0) = 0, \quad (11c)$$

$$\dot{K} = 0, \quad K_0(0) = K_0, \quad (11d)$$

$$\dot{n} = 0, \quad n(0) = n_0, \quad (11e)$$

$$J = J(x_3, J_0(c_1, c_2), K, n) \quad (11f)$$

or

$$\dot{\tilde{\mathbf{x}}} = \tilde{\mathbf{f}}(\tilde{\mathbf{x}}, \mathbf{u}). \quad (12)$$

Possible candidates for the process outputs are the concentrations c_1 , c_2 , and the permeate flux J . Observability matrix for such process description has rank equal to 4. This shows that parameters K and n are not simultaneously observable as they enter the process equations via J only and there are infinitely many combinations of them that can lead to the actual value of J .

A possible remedy is to add some new measured variable that is a different function of unknown parameters. One candidate is derivative \dot{J} of the flux with respect to time. Process observability is then of full rank. It is, however, not possible to measure \dot{J} exactly and we use an approximation of the third order to obtain its value.

It has to be noted that the structural identifiability of the parameters K and n was also confirmed by the Taylor series method (Pohjanpalo, 1978). However, this approach assumes idealized conditions (e.g., continuous measurements and the availability of the output signal and all its derivatives).

Process outputs measured in discrete-time samples are then given as

$$\mathbf{y}_k = \mathbf{h}(\mathbf{x}_k) = (c_1, c_2, x_3, J, \dot{J})^T. \quad (13)$$

The observer dynamics is given by

$$\dot{\hat{\mathbf{x}}} = \tilde{\mathbf{f}}(\hat{\mathbf{x}}, \mathbf{u}), \quad (14)$$

$$\dot{\mathbf{P}}^- = \mathbf{F}\mathbf{P}^- + \mathbf{P}^- \mathbf{F}^T + \mathbf{Q}, \quad (15)$$

for $t \in (t_{k-1}, t_k]$ with $\mathbf{P}^-(t_{k-1}) = \mathbf{P}_{k-1}^+$ and with the update of the observer defined as follows

$$\mathbf{L}_k = \mathbf{P}_k^- \mathbf{C}_k^T (\mathbf{C}_k \mathbf{P}_k^- \mathbf{C}_k^T + \mathbf{R}_k)^{-1}, \quad (16a)$$

$$\hat{\mathbf{x}}_k = \hat{\mathbf{x}}_{k-1} + \mathbf{L}_k (\mathbf{y}_k - \mathbf{h}(\hat{\mathbf{x}}_{k-1})), \quad (16b)$$

$$\mathbf{P}_k^+ = (\mathbf{I} - \mathbf{L}_k \mathbf{C}_k) \mathbf{P}_k^-, \quad (16c)$$

where the state transition and observation matrices are defined by following Jacobians

$$\mathbf{F} = \left. \frac{\partial \tilde{\mathbf{f}}}{\partial \tilde{\mathbf{x}}} \right|_{\hat{\mathbf{x}}(t), \mathbf{u}(t)}, \quad \mathbf{C}_k = \left. \frac{\partial \mathbf{h}}{\partial \tilde{\mathbf{x}}} \right|_{\hat{\mathbf{x}}_k}. \quad (17)$$

Matrices \mathbf{R} and \mathbf{Q} denote, respectively, the covariance matrix of the noise affecting the measurements and the

covariance matrix of the noise affecting the state dynamics. The matrix \mathbf{P} represents the covariance of the estimation error of states and parameters. The matrices \mathbf{R} , \mathbf{Q} and \mathbf{P}_0^+ can also be thought of as tuning knobs of the estimation algorithm affecting its estimation performance and convergence.

Based on the measured outputs the Kalman filter provides on-line estimates of parameters K and n . This knowledge is then used to update regions and parameters of the time-optimal controller.

5. CASE STUDY

We consider the batch membrane process which operates under limiting flux conditions. The permeate flux of the unfouled membrane is then as follows

$$J_0(c_1) = k \ln \left(\frac{c_{\text{lim}}}{c_1} \right), \quad (18)$$

where k is the mass transfer coefficient and c_{lim} is the limiting concentration of the macro-solute. We can observe that the permeate flux depends solely on the macro-solute concentration. The goal is to drive the system from initial concentrations $[c_{1,0}, c_{2,0}] = [10 \text{ mol/m}^3, 100 \text{ mol/m}^3]$ to final concentrations $[c_{1,f}, c_{2,f}] = [100 \text{ mol/m}^3, 1 \text{ mol/m}^3]$ in minimum time. The initial volume of the filtered solution is $V_0 = 100 \text{ L}$. We consider the limiting flux model with parameters $k = 4.79 \text{ m/s}$, $c_{\text{lim}} = 319 \text{ mol/m}^3$ and the membrane area 1 m^2 .

Three simulation experiments were performed with one constant value of the fouling rate $K = 2$ and different values of n , hence with different fouling models.

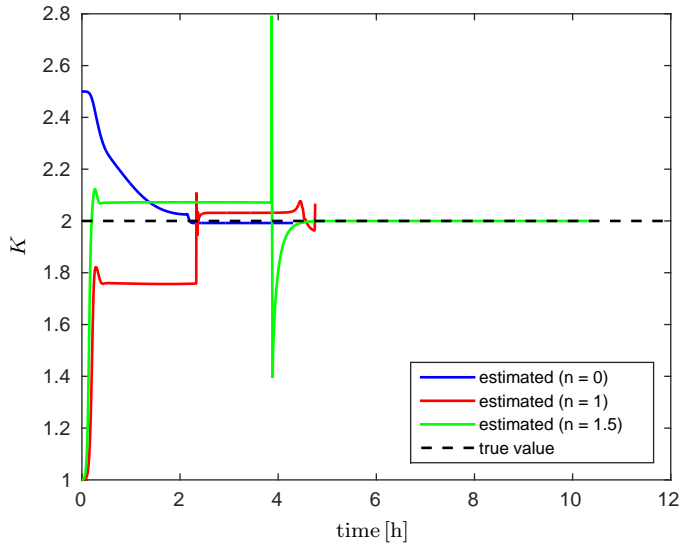
A crucial point in the design of an EKF is the choice of the covariance matrices that affect the performance and the convergence of EKF. In this preliminary study we did not consider any measurement noise therefore we chose the matrix $\mathbf{R} = 0.001 \mathbf{I}_5$. The initial estimation error for the states and the estimated parameters represented by matrix \mathbf{P}_0 is of the following form

$$\mathbf{P}_0 = \text{diag}(0.001, 0.001, 0.001, 0.1, 0.1), \quad (19)$$

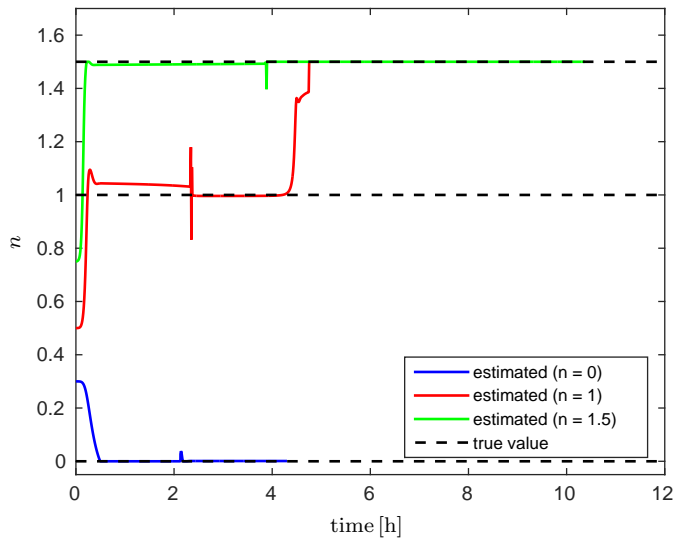
where we assume that the initial measurement error for the first three states is small since the concentrations are known. Similarly, the covariance matrix which affects the state dynamics \mathbf{Q} is chosen as follows

$$\mathbf{Q} = \text{diag}(0.001, 0.001, 0.001, 100, 20). \quad (20)$$

Time evolutions of the parameter estimates for the individual fouling models are shown in Fig. 3. Although the estimated values of the parameters do not converge exactly to the true values, they are, in all cases, reasonably close to them. This is mainly caused by the approximation of the derivative of the flux and by nonlinearity of the process model. The convergence is always achieved within the first control arc (concentration mode) of the operation where the control is constant and does not depend on estimated parameters or the states variables. Fouling parameter estimates are needed to accurately estimate the time of switching to the second control arc and to calculate the singular control. Therefore, as the Kalman filter can converge to the neighborhood of true parameters within the first mode, the proposed procedure yields all considered simulation scenarios having practically the same



(a) Estimation of the fouling parameter K .



(b) Estimation of the fouling parameter n .

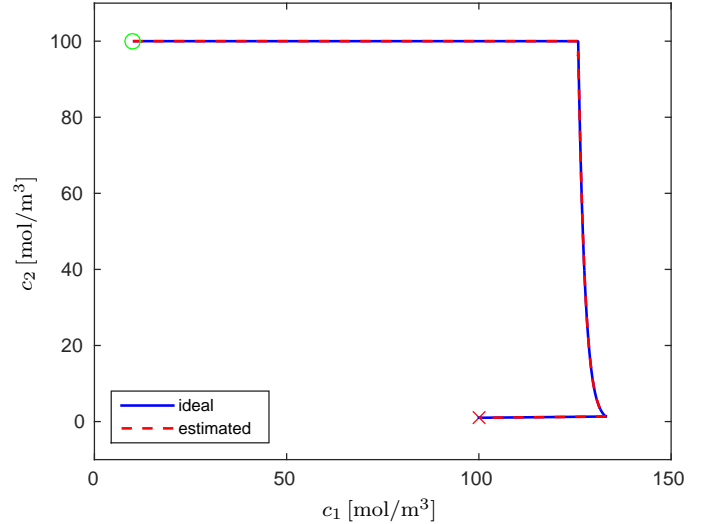
Fig. 3. Estimation of the fouling parameter n for the three chosen cases.

performance as the optimal control with perfect knowledge of the fouling model and its parameters.

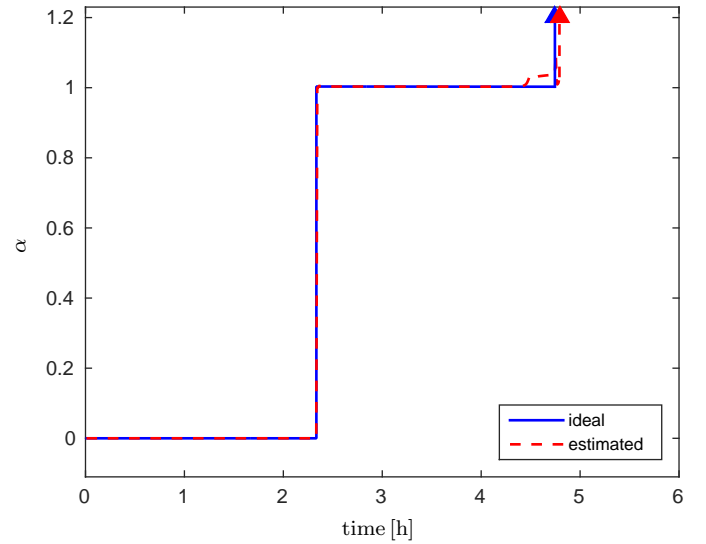
We can observe oscillations of parameter values around the first and the second switching times. In the intermediate fouling model, n actually diverged near the second switch. This is caused by the approximation of \dot{J} as it does not occur when the true value of \dot{J} was used as the measured value.

Parameter estimation can be terminated after the second switch. Control in the third arc is given by $\alpha = \infty$ and this control mode is performed after the separation – we only add water to reach the desired final concentrations.

Fig. 4 shows the ideal optimal concentration state diagram and corresponding optimal control profile (blue line) for the case with perfect knowledge of fouling parameters ($K = 2$ and $n = 1$). The dashed red line represents the behavior of the concentrations and the control profile with



(a) Concentration state diagram



(b) Optimal control profile

Fig. 4. Concentration state diagram and optimal control profile for ideal and estimated fouling parameters ($K = 2$ and $n = 1.5$).

estimated fouling parameters. We note that this was the worst case of the three with parameter convergence issues.

As explained in the theoretical part, the optimal operation is a three step strategy $\alpha = (0, \alpha_2(t), \infty)$ where the second step is the singular control close to one (for this membrane and the fouling model). Difference in optimal switching times and switching concentrations stay below 1%. The largest difference in the control profile is 4% before the second switch. However, as it occurs only during the last few minutes of the separation it has only a minor impact on the state/control profiles and on the operating time.

6. CONCLUSIONS

In this paper we studied the time-optimal operation of a general batch diafiltration process in the presence of membrane fouling. The time-optimal operation and control can be described as an explicit nonlinear optimal control law defined over state regions. The structure of the optimal

operation consists generally of three steps with a singular control in the middle step.

The Extended Kalman Filter was proposed to estimate the main parameters that describe the fouling behavior. The main motivation was to estimate the fouling parameters directly during the separation process. Online estimation can be crucial as the fouling can change during the run. The results indicate that the EKF is able to converge to the neighborhood of true values of the fouling parameters. The convergence is satisfactory even if the control variable is constant during the first time interval and does not guarantee persistent excitation conditions. Therefore, it is possible to predict the fouling mechanism during the run of the process.

Further research directions will be focused on experimental verification of the proposed procedure in laboratory conditions.

ACKNOWLEDGEMENTS

The authors gratefully acknowledge the contribution of the Scientific Grant Agency of the Slovak Republic under the grant 1/0053/13, the Slovak Research and Development Agency under the project APVV-0551-11 and the internal grant of the Slovak University of Technology in Bratislava. This contribution/publication is also the partial result of the Research & Development Operational Programme for the project University Scientific Park STU in Bratislava, ITMS 26240220084, supported by the Research 7 Development Operational Programme funded by the ERDF. The fourth, fifth and sixth author is grateful for the KUL PFV/10/002 (OPTEC) grant.

REFERENCES

- Abbasi, M., Sebzari, M.R., Salahi, A., and Mirza, B. (2012). Modeling of membrane fouling and flux decline in microfiltration of oily wastewater using ceramic membranes. *Chemical Engineering Communications*, 199(1), 78–93.
- Alessandri, A., Baglietto, M., and Battistelli, G. (2005). Robust receding-horizon state estimation for uncertain discrete-time linear systems. *Systems & Control Letters*, 54(7), 627 – 643.
- Bavdekar, V.A., Deshpande, A.P., and Patwardhan, S.C. (2011). Identification of process and measurement noise covariance for state and parameter estimation using extended Kalman filter. *Journal of Process Control*, 21(4), 585 – 601. doi: <http://dx.doi.org/10.1016/j.jprocont.2011.01.001>.
- Bolton, G., LaCasse, D., and Kuriyel, R. (2006). Combined models of membrane fouling: Development and application to microfiltration and ultrafiltration of biological fluids. *Journal of Membrane Science*, 277(1–2), 75 – 84. doi: <http://dx.doi.org/10.1016/j.memsci.2004.12.053>.
- Bryson, Jr., A.E. and Ho, Y.C. (1975). *Applied Optimal Control*. Taylor & Francis Group, New York, USA, 2 edition.
- Charfi, A., Amar, N.B., and Harmand, J. (2012). Analysis of fouling mechanisms in anaerobic membrane bioreactors. *Water Research*, 46(8), 2637 – 2650. doi: <http://dx.doi.org/10.1016/j.watres.2012.02.021>.
- Cheryan, M. (1998). *Ultrafiltration and Microfiltration Handbook*. CRC Press, Florida, USA.
- Foley, G. (1999). Minimisation of process time in ultrafiltration and continuous diafiltration: the effect of incomplete macrosolute rejection. *Journal of Membrane Science*, 163(1–2), 349–355.
- Hermia, J. (1982). Constant pressure blocking filtration laws-application to power-law non-Newtonian fluids. *Transactions of the Institution of Chemical Engineers*, 60(183).
- Jelemenský, M., Sharma, A., Paulen, R., and Fikar, M. (2015a). Time-optimal control of batch multi-component diafiltration processes. In *25th European Symposium on Computer Aided Process Engineering*, 1577–1582. Copenhagen, Denmark.
- Jelemenský, M., Sharma, A., Paulen, R., and Fikar, M. (2015b). Time-optimal operation of diafiltration processes in the presence of fouling. In K.V. Gernaey, J.K. Huusom, and R. Gani (eds.), *12th International Symposium on Process Systems Engineering And 25th European Symposium on Computer Aided Process Engineering*, 1577–1582. Elsevier B.V, Copenhagen, Denmark.
- Kalman, R.E. (1960). A new approach to linear filtering and prediction problems. *Transactions of the ASME—Journal of Basic Engineering*, 82(Series D), 35–45.
- Kovács, Z., Fikar, M., and Czermak, P. (2009). Mathematical modeling of diafiltration. In *Conference of Chemical Engineering*, 135–135. Pannonia University, Veszprem.
- Ng, P., Lundblad, J., and Mitra, G. (1976). Optimization of Solute Separation by Diafiltration. *Separation Science and Technology*, 11(5), 499–502.
- Paulen, R., Fikar, M., Foley, G., Kovács, Z., and Czermak, P. (2012). Optimal feeding strategy of diafiltration buffer in batch membrane processes. *Journal of Membrane Science*, 411-412, 160–172. doi: 10.1016/j.memsci.2012.04.028.
- Paulen, R., Jelemenský, M., Kovacs, Z., and Fikar, M. (2015). Economically optimal batch diafiltration via analytical multi-objective optimal control. *Journal of Process Control*, 28, 73–82.
- Pohjanpalo, H. (1978). System identifiability based on the power series expansion of the solution. *Mathematical Biosciences*, 41(12), 21 – 33. doi: [http://dx.doi.org/10.1016/0025-5564\(78\)90063-9](http://dx.doi.org/10.1016/0025-5564(78)90063-9).
- Pontryagin, L.S., Boltyanskii, V.G., Gamkrelidze, R.V., and Mishchenko, E.F. (1962). *The Mathematical Theory of Optimal Processes*. New York, USA.
- Salahi, A., Abbasi, M., and Mohammadi, T. (2010). Permeate flux decline during UF of oily wastewater: Experimental and modeling. *Desalination*, 251(1-3), 153–160.
- Takači, A., Žikić-Došenović, T., and Zavargó, Z. (2009). Mathematical model of variable volume diafiltration with time dependent water adding. *Engineering Computations: International Journal for Computer-Aided Engineering and Software*, 26(7), 857–867.
- Vela, M.C.V., Blanco, S.A., García, J.L., and Rodríguez, E.B. (2008). Analysis of membrane pore blocking models applied to the ultrafiltration of {PEG}. *Separation and Purification Technology*, 62(3), 489 – 498. doi: <http://dx.doi.org/10.1016/j.seppur.2008.02.028>.